

Mean field approaches to the totally asymmetric exclusion process with quenched disorder and large particles

Leah B. Shaw,^{1,2,*} James P. Sethna,¹ and Kelvin H. Lee²

¹*Department of Physics, Cornell University, Ithaca, NY 14853-2501*

²*School of Chemical and Biomolecular Engineering, Cornell University, Ithaca, NY 14853-5201*

(Dated: August 16, 2018)

The process of protein synthesis in biological systems resembles a one dimensional driven lattice gas in which the particles (ribosomes) have spatial extent, covering more than one lattice site. Realistic, nonuniform gene sequences lead to quenched disorder in the particle hopping rates. We study the totally asymmetric exclusion process with large particles and quenched disorder via several mean field approaches and compare the mean field results with Monte Carlo simulations. Mean field equations obtained from the literature are found to be reasonably effective in describing this system. A numerical technique is developed for computing the particle current rapidly. The mean field approach is extended to include two-point correlations between adjacent sites. The two-point results are found to match Monte Carlo simulations more closely.

PACS numbers: 82.39.-k, 05.10.-a

Introduction

The process of protein synthesis, called “translation,” can be modeled using a driven lattice gas in one dimension [1, 2, 3, 4]. This type of model is well understood when all particle hopping rates are uniform, but a model for the real biological process requires nonuniform particle hopping rates. Direct Monte Carlo simulation of such models is possible when only a few genes are involved. However, it is desirable to perform large-scale simulations to fit translation models to experimental data collected for many genes simultaneously (e.g., data from [5]). For this purpose, Monte Carlo approaches would be computationally too slow. Therefore, other analytical or computational methods are needed.

In this paper, we address the issue of quenched disorder (site-dependent hopping rates) in a driven lattice gas model for translation. The paper is organized as follows. The model is first described and its connection to biological protein synthesis explained. Section II contains a brief summary of known results. In Section III, we use a simple coarse-grained approach to obtain crude, approximate solutions. Section IV treats our central topic: application of a mean field method [1, 2] to the problem of quenched disorder. Analytical and computational results are presented. In Section V, we extend the mean field approach to include two-point correlations for better accuracy. We close with a brief summary and discussion of how these methods may be applied to problems of interest, such as fitting translation models to experimental data.

I. DESCRIPTION OF MODEL

We focus on translation in prokaryotes, particularly *Escherichia coli*, because of its relative simplicity. The process involves the synthesis of specific proteins based on the sequence of messenger RNA (mRNA) molecules. The mechanism consists of ribosomes “reading” the codons of mRNA as the ribosomes move along an mRNA chain, and the recruitment and assembly of amino acids (appropriate to the codons being read) to form a protein. (See, e.g., [6], for more details.) This process is often described as three steps: initiation, where ribosomes attach themselves, one at a time, at the “start” end of the mRNA; elongation, where the ribosomes move down the chain in a series of steps; and termination, where they detach at the “stop” codon. Since ribosomes cannot overlap, their dynamics is subject to the excluded volume constraint. Apart from being impeded by another ribosome (steric hinderance), a ribosome cannot move until the arrival of an appropriate transfer RNA, carrying the appropriate amino acid (a combination known as aminoacyl-tRNA, or aa-tRNA). Thus, the relative abundances of the approximately 60 types [7] of aa-tRNA have significant effects on the elongation rate. Assuming reactant availabilities in a cell are in their steady state, with a time-independent concentration of ribosomes and aa-tRNA, there would be an approximately steady current of ribosomes moving along the mRNA, resulting in a specific production rate of this particular protein. Our goal is the prediction of the protein production rates for various mRNA’s, as a function of the concentration of ribosomes and aa-tRNA’s.

The process of translation is well suited to modeling using a driven lattice gas in one dimension. Particles enter at some rate on one end of a chain of discrete lattice sites (initiation), then hop down the chain one site at a time with another rate or set of rates (elongation), and finally exit the chain at the other end (termination).

*Electronic address: lbs22@cornell.edu

The excluded volume constraint is implemented by insuring the spacing between ribosomes is no less than 12 sites, the approximate number of codons that a ribosome blocks [8, 9]. Quenched disorder arises because there is non-uniformity in the hopping (elongation) rates along the chain. This effect occurs because at each codon, a ribosome has to “wait” for the appropriate aa-tRNA before continuing, and the various aa-tRNA’s are present in nonequal abundances.

The model we employ is the same as in [4]. We model an mRNA with N codons as a chain of sites, each of which is labeled by i . The first and last sites, $i = 1, N$, are associated with the start and stop codons, respectively. At any time, attached to the mRNA are M ribosomes (particles). Being a large complex of molecules, each ribosome will cover ℓ sites (codons), with $\ell = 12$ typically [8, 9]. Any site may be covered by a single ribosome or none. In case of the latter, we will refer to the site as “empty” or “occupied by a hole.” To locate the ribosome, we arbitrarily choose the *lowest* site covered. For example, if the first ℓ sites are empty, a ribosome can bind in an initiation step, and then it is said to be “on site $i = 1$.” We define n_i to be the ribosome density at site i , where only the left end of the ribosome is counted. (In [1, 2], particles were located by their right end, but either choice leads to the same rules of motion.) We also define the coverage density $\rho_i = \sum_{s=0}^{\ell-1} n_{i-s}$, which is the probability that site i is covered by some portion of a ribosome.

Next, we specify the dynamics of our model. An attached ribosome located at site i will move to the next site ($i + 1$) with a rate k_i , provided site $i + \ell$ is empty. For Monte Carlo simulations, it is convenient to update configurations in discrete time units Δt . In implementing the simulations, it is better to use probabilities $p_i = k_i \Delta t$, so that a ribosome on site i will be moved (or not) with probability p_i (or $1 - p_i$). We purposefully associate these hopping probabilities with a site because a site is associated with a particular codon. Thus, the hopping rate from that site may depend on the relative abundance of the appropriate aa-tRNA. Apart from these probabilities, another aspect of our simulations is random sequential updating: i.e., during each Monte Carlo step (MCS), $M + 1$ particles are chosen at random, in sequence, to attempt moves. They are selected from a pool that includes the M particles on the lattice plus another unbound particle that can initiate if there are ℓ holes at the beginning of the chain.

In our computational studies, systems begin empty and are run for long enough to reach steady state. After steady state is attained, data including the current and density distribution can be collected. Density data is typically collected every 100 MCS. We often use continuous time Monte Carlo [10] because it runs far more quickly than and provides the same results as standard Monte Carlo. Using continuous time Monte Carlo also avoids the need to specify a fixed time step Δt .

In our studies of real mRNA sequences, we use gene se-

quences from *Escherichia coli* strain MG1655, obtained from [11]. Elongation rates at each codon are estimated using commonly accepted values for the availability of tRNA in *E. coli* [12]. The rate at each codon is assumed proportional (with an arbitrary proportionality constant) to the availability of the appropriate tRNA that can decode the codon, as in [13]. Corresponding data are not available for estimating initiation and termination rates, so we choose various rates of interest to study.

II. SUMMARY OF PREVIOUS RESULTS

Extensive investigations of the simple totally asymmetric exclusion process (TASEP, defined as point particles hopping with unit rate along a line) with open boundaries can be found in the literature. We first consider studies of uniform systems. Exact analytic results for the $\ell = 1$ steady state exist [14, 15]. Systems with extended objects ($\ell > 1$) have been less frequently investigated but have also been understood from various approaches. Using a mean field approach, MacDonald *et al.* derived mean field equations for the average site occupation $\langle n_i \rangle$ and considered both closed [1] and open [2] systems. In the former case, exact solutions were found, leading to a current vs. density relation. For the latter, the authors resorted to numerical solutions to find the phase diagram for a variety of initiation and termination rates. Lakatos and Chou [3] considered uniform open systems with extended objects. Using a discrete Tonks gas partition function, they derived the current vs. density relation first presented by MacDonald *et al.* [1]. Via a refined mean field theory, they extended this result to predict currents and bulk densities for the open system, which they confirmed by Monte Carlo simulations. Finally, Shaw *et al.* [4] used an extremal principle [16] based on domain wall theory [17] to obtain the phase diagram, with currents and bulk densities, for the uniform open system. They also found approximate density profiles (related to the coverage density ρ) from a continuum limit. From all of these studies, the $\ell > 1$ phase diagram is well known. Depending on the initiation (or injection) and termination (or depletion) rates, the system will settle into one of three phases. From their dominant characteristics, the three phases are known as low density, high density, and maximal current. The initiation and termination probabilities are often referred to as α and β in the literature. A phase diagram in this α - β plane has been determined, showing second order transitions between the maximal current phase and the others, as well as a first order transition between the high- and low-density regions.

When disorder is introduced, i.e., not all the p_i ’s are equal, then methods for exact analytic approaches fail (except in the extremely dilute limit, where only the motion of a single particle is of concern [18]). Indeed, even a single slow rate in a *closed* system poses serious difficulties [19, 20, 21]. However, Kolomeisky [22] obtained

approximate steady state solutions and phase diagrams for an *open* system with a single nonuniform rate in the bulk by splitting the system into two smaller systems connected by the nonuniform rate. Tripathy and Barma [23] considered a closed system, but with a finite fraction of identical slow sites. Based on a combination of Monte Carlo simulations and numerical solutions of mean field equations, they found current-density relations. Further references on TASEP with disorder may be found in a recent review [24]. All of these studies are restricted to $\ell = 1$. Studies of disorder in systems with $\ell > 1$ have been fairly limited. Shaw *et al.* [4] found upper and lower bounds for the current in systems with arbitrary disorder. In another work, Shaw *et al.* [25] considered an open system with $\ell > 1$ and a single nonuniform rate in the bulk. As was done for $\ell = 1$ [22], the system was divided into two smaller systems connected by the nonuniform rate. Steady state currents and bulk densities to either side of the nonuniform site were obtained.

III. SIMPLE COARSE-GRAINING APPROACH

We consider briefly an approximate method motivated by the method of Shaw *et al.* [25]. Their particle hopping rate in the bulk was 1, except for the nonuniform rate q at special site k . Important in their analysis is the parameter

$$q_{eff} = \frac{\ell}{1/q + (\ell - 1)}.$$

This parameter appears in the current passing from the left sublattice into the right sublattice:

$$J = q_{eff} \frac{\rho_{left}}{\ell} \frac{(1 - \rho_{right})}{(1 - \rho_{right} + \rho_{right}/\ell)}, \quad (1)$$

where ρ_{left} and ρ_{right} are the bulk densities in the left and right sublattices. We note that q_{eff} is the same as $\ell K_{\ell,k}$ in the notation of [4], where

$$K_{\ell,i} \equiv \left(\sum_{j=i}^{i+\ell-1} \frac{1}{k_j} \right)^{-1}$$

is a coarse-grained rate for translating ℓ sites.

The form of Eq. 1 motivates us to suggest that

$$J = \ell K_{\ell,i} \frac{\rho_i}{\ell} \frac{1 - \rho_i}{1 - \rho_i + \rho_i/\ell} \quad (2)$$

in regimes in which the coverage density ρ is slowly varying in i . Because ρ and K_ℓ are both coarse-grained over a distance ℓ , a relationship between them is unsurprising. Eq. 2 can be solved for ρ_i :

$$\rho_i = \frac{1}{2K_{\ell,i}} \left[K_{\ell,i} + J - J/\ell \pm \sqrt{(K_{\ell,i} + J - J/\ell)^2 - 4JK_{\ell,i}} \right] \quad (3)$$

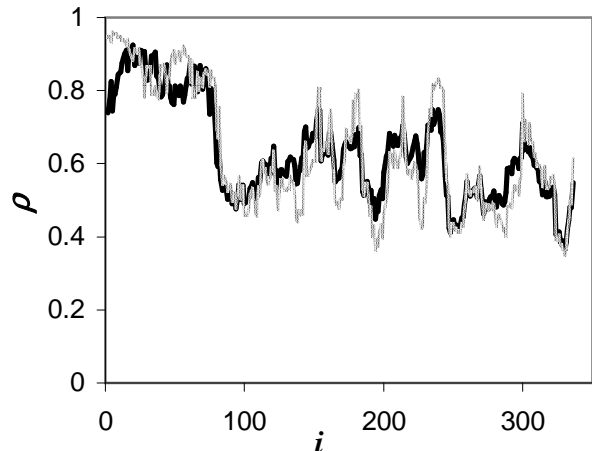


FIG. 1: Coverage density profile for the *ompA* gene of *E. coli* when elongation rates are limiting. Bold curve is Monte Carlo simulation result, and lighter curve is coarse-grained prediction from Eq. 3 using the Monte Carlo current. The positive root was used to the left of the current-limiting region and the negative root to the right. The real part is plotted where the predicted ρ is complex. Elongation rates at each codon were assumed proportional to availabilities of corresponding tRNA [12].

It is reasonable to use the positive (high density) root to the left of the current-limiting region (where the minimum K_ℓ occurs) and the negative (low density) root to the right. Results of this approach are shown in Fig. 1 for the *ompA* gene when elongation rates are limiting (i.e., initiation and termination rates are sufficiently large). The value for current J in Eq. 3 is taken from Monte Carlo simulations of *ompA*. The agreement between the coarse-grained result and Monte Carlo simulations is good in low density regions but is poorer in high density regions because long range correlations become more important, an effect not captured by coarse-graining over the relatively short distance ℓ . Finally, we note that Eq. 3 can be used only when the current J is known, either from Monte Carlo simulations or from some analytical means.

IV. MEAN FIELD APPROACH

We next turn to a mean field approach, using equations first developed by MacDonald *et al.* [1, 2]. The equations were applied only to uniform systems, but we will find that they can be successfully applied to nonuniform systems. Here the location of a particle is determined by the location of its left end. The particle density at site i is n_i , and the hole density at site i is $1 - \sum_{s=0}^{\ell-1} n_{i-s}$. For a particle to move from site i to $i+1$, producing a current, site $i+\ell$ must be empty. The method is “mean field” in the sense that some correlations have been neglected. The conditional probability that site $i+\ell$ is empty given that site i contains a particle is replaced by the condi-

tional probability that site $i + \ell$ is empty given that site i contains either a particle or a hole. That is,

$$\begin{aligned} P(\bullet - \circ \mid \bullet - ?) &= \frac{P(\bullet - \circ)}{P(\bullet - \circ) + P(\bullet - \bullet)} \\ &\approx P(? - \circ \mid ? - ?) \\ &= \frac{P(\bullet - \circ) + P(\circ - \circ)}{P(\bullet - \circ) + P(\bullet - \bullet) + P(\circ - \circ) + P(\circ - \bullet)} \\ &= \frac{1 - \sum_{s=1}^{\ell} n_{i+s}}{1 - \sum_{s=1}^{\ell} n_{i+s} + n_{i+\ell}}, \end{aligned}$$

where we use \bullet to denote a filled site and \circ to denote an empty site.

The mean field assumption for the conditional probability leads to the following equations for the time evolution of the $\{n_i\}$:

$$\begin{aligned} \frac{dn_1}{dt} &= k_0 \left(1 - \sum_{s=1}^{\ell} n_s\right) - k_1 n_1 \frac{1 - \sum_{s=1}^{\ell} n_{1+s}}{1 - \sum_{s=1}^{\ell} n_{1+s} + n_{1+\ell}} \\ \frac{dn_i}{dt} &= k_{i-1} n_{i-1} \frac{1 - \sum_{s=1}^{\ell} n_{i-1+s}}{1 - \sum_{s=1}^{\ell} n_{i-1+s} + n_{i-1+\ell}} - k_i n_i \frac{1 - \sum_{s=1}^{\ell} n_{i+s}}{1 - \sum_{s=1}^{\ell} n_{i+s} + n_{i+\ell}} \text{ for } i = 2, \dots, N - \ell \\ \frac{dn_{N-\ell+1}}{dt} &= k_{N-\ell} n_{N-\ell} \frac{1 - \sum_{s=1}^{\ell} n_{N-\ell+s}}{1 - \sum_{s=1}^{\ell} n_{N-\ell+s} + n_N} - k_{N-\ell+1} n_{N-\ell+1} \\ \frac{dn_i}{dt} &= k_{i-1} n_{i-1} - k_i n_i \text{ for } i = N - \ell + 2, \dots, N, \end{aligned} \quad (4)$$

where we use k_0 to denote the initiation rate.

For the steady state solution, time derivatives are set to 0 and the current J is introduced. The resulting set of equations,

$$J = k_0 \left(1 - \sum_{s=1}^{\ell} n_s\right) \quad (5a)$$

$$n_i = \frac{J}{k_i} \frac{1 - \sum_{s=1}^{\ell} n_{i+s} + n_{i+\ell}}{1 - \sum_{s=1}^{\ell} n_{i+s}} \text{ for } i = 1, \dots, N - \ell \quad (5b)$$

$$n_i = \frac{J}{k_i} \text{ for } i = N - \ell + 1, \dots, N, \quad (5c)$$

can be solved iteratively for n_N to n_1 if J is specified. Then Eq. 5a becomes an initial condition to check for consistency to determine whether J has been chosen correctly. If Eq. 5a is not satisfied, then J should be adjusted appropriately and the process repeated.

We present an argument for the validity of this it-

erative approach. First, a physically meaningful solution will have particle density $n_i \in (0, 1)$ and coverage density $\sum_{s=1}^{\ell} n_{i+s} \in (0, 1)$ for all i . (Endpoints of the interval are excluded if there is to be nonzero current flow.) Suppose that for some i , $J > k_i(1 - \sum_{s=1}^{\ell} n_{i+s})$. Then from Eq. 5b, $n_i > 1 - \sum_{s=1}^{\ell-1} n_{i+s}$, meaning that $\sum_{s=0}^{\ell-1} n_{i+s} > 1$, which is a contradiction. So we see that $J \leq k_i(1 - \sum_{s=1}^{\ell} n_{i+s})$ for all i . (Note that although we have not dealt separately with $i = N - \ell + 1, \dots, N$, Eq. 5c is consistent with the previous statement.) Thus, J cannot be too large if physical solutions are to be obtained.

Next, we show that the densities $\{n_i\}$, while within physical ranges, are increasing functions of J . Consider two different J values: J_0 with its associated densities $\{n_i\}$ and J_1 with its densities $\{m_i\}$, which we assume to be in physical ranges. Suppose that $J_1 > J_0$. Clearly $m_i > n_i$ for $i = N - \ell + 1, \dots, N$. Using induction on the remaining i , it can be shown from Eq. 5b that

$$\begin{aligned} m_i - n_i &> \frac{J_0}{k_i} \frac{1 - \sum_{s=1}^{\ell} m_{i+s} + m_{i+\ell}}{1 - \sum_{s=1}^{\ell} m_{i+s}} - \frac{J_0}{k_i} \frac{1 - \sum_{s=1}^{\ell} n_{i+s} + n_{i+\ell}}{1 - \sum_{s=1}^{\ell} n_{i+s}} \\ &= \frac{J_0}{k_i \left(1 - \sum_{s=1}^{\ell} m_{i+s}\right) \left(1 - \sum_{s=1}^{\ell} n_{i+s}\right)} \left[m_{i+\ell} \left(1 - \sum_{s=1}^{\ell} n_{i+s}\right) - n_{i+\ell} \left(1 - \sum_{s=1}^{\ell} m_{i+s}\right) \right] \\ &> 0. \end{aligned}$$

Therefore, the densities $\{n_i\}$ increase with increasing J .

Finally, we again consider Eq. 5a. The left side increases monotonically with increasing J , and the right decreases monotonically with increasing J , while densities are in physical ranges. If we follow the iterative approach, J values that lead to $\sum_{s=1}^{\ell} n_{i+s} > 1$ or $J > k_0 \left(1 - \sum_{s=1}^{\ell} n_s\right)$ are too large and should be decreased. On the other hand, J values that lead to $J < k_0 \left(1 - \sum_{s=1}^{\ell} n_s\right)$ are too small and should be increased. One can start with upper and lower bounds for the current (from [4]) and use bisection to converge to the correct current. If a physical solution exists, it is unique and should be found by this method.

Note that the upper bound for J from [4],

$$J \leq \left(\sum_{s=0}^{\ell-1} \frac{1}{k_{i+s}} \right) \quad (6)$$

for all i , applies also to the mean field equations. This can be shown from

$$\begin{aligned} \sum_{s=1}^{\ell} \frac{J}{k_{i+s}} &= \sum_{s=1}^{\ell} n_{i+s} \frac{1 - \sum_{t=1}^{\ell} n_{i+s+t}}{1 - \sum_{t=1}^{\ell} n_{i+s+t} + n_{i+s+\ell}} \\ &\leq \sum_{s=1}^{\ell} n_{i+s} \leq 1. \end{aligned}$$

In practice, computing iterative solutions for $\{n_i\}$ and adjusting J by bisection is effective in finding J and finding n_i values that are low density (downstream of the current-limiting region). Table I shows that there is fairly good agreement (within 5%) between the mean field current and the actual current (from Monte Carlo simulations) for various real gene sequences of *E. coli*. However, numerical problems arise in finding n_i values that are high density (upstream of the current-limiting region). For high density solutions, we have observed that there generally exists a very narrow range for J , with a width less than machine precision, for which the smaller J values will fail to satisfy Eq. 5a because the densities are too small, and for which the larger J values will lead to nonphysical densities. An example of this phenomenon is shown in Fig. 2.

We next present an argument for why high density solutions are associated with numerical difficulties. For convenience, we assume that the k_i are uniformly 1, and we seek uniform density solutions. Eq. 5b gives an iterative map for n_i . We assume that a fixed point n^* exists. It will then satisfy

$$n^* = J \frac{1 - (\ell - 1)n^*}{1 - \ell n^*}.$$

We find high density and low density fixed points,

$$n_{\pm}^* = \frac{1}{2\ell} \left[1 + J(\ell - 1) \pm \sqrt{[1 + J(\ell - 1)]^2 - 4\ell J} \right].$$

TABLE I: Currents for real gene sequences of *E. coli* from Monte Carlo (MC) simulations and mean field (MF) calculations. Both the original mean field and the two-point mean field are included. Units for the currents are arbitrary. Percent errors for the mean field currents, as compared with the Monte Carlo currents, are given in parentheses. Elongation rates were assumed proportional to the availability of the appropriate tRNA for each codon [12]. Several of the genes were chosen to be initiation-limited by making the initiation rate 0.78 of the slowest elongation rate. Others were made termination-limited by making the termination rate 0.34 (for *asnS* and *envY*) or 0.52 (for *fabG*) of the slowest elongation rate. The remainder were elongation-limited. Errors in the Monte Carlo results are less than 0.001.

gene	limit	MC J	orig. MF J (%err)	2-pt. MF J (%err)
adk	elong.	0.139	0.133 (4.3)	0.137 (1.4)
cysK	elong.	0.120	0.122 (1.7)	0.118 (1.7)
gapA	elong.	0.194	0.191 (1.5)	0.191 (1.5)
glnH	elong.	0.156	0.154 (1.3)	0.158 (1.3)
aceF	init.	0.170	0.164 (3.5)	0.166 (2.4)
crr	init.	0.172	0.177 (2.9)	0.172 (0.0)
fabD	init.	0.114	0.112 (1.8)	0.112 (1.8)
asnS	term.	0.114	0.114 (0.0)	0.114 (0.0)
envY	term.	0.092	0.091 (1.1)	0.091 (1.1)
fabG	term.	0.112	0.113 (0.9)	0.112 (0.0)

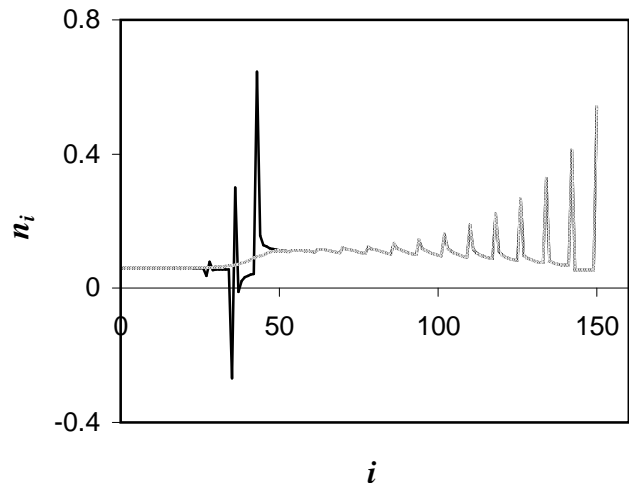


FIG. 2: Particle density profiles calculated by iteration of mean field equations (Eq. 5) for a uniform system with initiation rate 1, elongation rates 1, and termination rate 0.1. The system had $N = 150$ and $\ell = 8$. The dark curve is the result for current J slightly too large, and the light/diffuse curve is the result for J slightly too small. The two curves are superimposed for $i > 50$. The difference between the two J values was $2 \times 10^{-19} J$.

Suppose the densities $n_{i+1}, \dots, n_{i+\ell}$ are slightly perturbed from the high density fixed point, so that $n_j =$

$n_+ + \delta$, where $|\delta| \ll 1$, for $j = i + 1, \dots, i + \ell$. Then

$$\begin{aligned} n_i &= J \frac{1 - (\ell - 1)n_+ - (\ell - 1)\delta}{1 - \ell n_+ - \ell \delta} \\ &= n_+ + \frac{4J}{\left[-1 + (\ell - 1)J + \sqrt{[1 + J(\ell - 1)]^2 - 4\ell J}\right]^2} \delta \\ &\quad + O(\delta^2). \end{aligned}$$

To determine stability of the high density fixed point, we consider the δ prefactor:

$$a \equiv \frac{4J}{\left[-1 + (\ell - 1)J + \sqrt{[1 + J(\ell - 1)]^2 - 4\ell J}\right]^2}$$

For currents in the expected range, $J \in (0, 1/(1 + \sqrt{\ell})^2)$ (cf. [2]), $a > 1$ so that the high density fixed point is unstable. A similar argument shows the stability of the low density fixed point. Although these ideas are proven here only for uniform density solutions, our numerical results (such as those in Fig. 2) lead us to believe that the nonuniform density case is similar. It appears that small numerical imprecisions prevent us from accurately finding high density solutions, while low density solutions can be easily found.

Finding steady state high density mean field solutions is a nontrivial problem. We have attempted multidimensional Newton's method approaches to solve Eq. 5 for $\{n_i\}$ and J , but these have their own difficulties. Convergence often fails unless the initial guess is very near the solution. The most reliable method is to start with an empty lattice and integrate Eq. 4 to steady state. Although integration is computationally slow, it consistently produces density profiles that are reasonable and similar to the Monte Carlo simulation density profiles. Agreement is best in the low density regime, when the correlations neglected by the mean field theory are less important (data not shown). In the high density regime, the mean field results underestimate the correlations between adjacent particles. An example of this discrepancy is shown for a uniform system in Fig. 3.

V. MEAN FIELD WITH TWO-POINT CORRELATIONS

To obtain more accurate solutions for density profiles, especially in the high density regime, we extend the mean field theory to include two-point correlations between adjacent sites. Variables in the two-point mean field theory are densities of bonds, indexed by i , where bond i connects site i to site $i + 1$. There are four types of bond densities, which we denote as follows: $n_{o,i}$, hole-hole pairs ($o-o$); $n_{\rightarrow,i}$, particle-hole pairs ($\bullet-o$); $n_{\leftarrow,i}$, hole-particle pairs ($o-\bullet$); and $n_{\times,i}$, particle-particle pairs ($\bullet-\bullet$). Geometry requires that

$$n_{\times,i} + n_{\leftarrow,i} = n_{\times,i+1} + n_{\rightarrow,i+1} \quad (7)$$

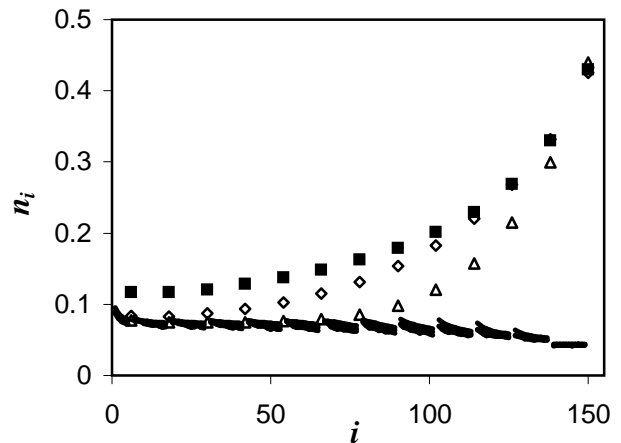


FIG. 3: Particle density profile for a uniform system with initiation rate 1, elongation rates 1, and termination rate 0.1. The system had $N = 150$ and $\ell = 12$. Density peaks (every ℓ sites) are displayed as symbols: filled squares are the Monte Carlo simulation result, open triangles are the prediction from the original mean field theory, and open diamonds are the prediction from the two-point mean field theory. Non-peak densities are displayed as curves; non-peak results from all three methods overlap.

and

$$n_{o,i} + n_{\rightarrow,i} = n_{o,i+1} + n_{\leftarrow,i+1}. \quad (8)$$

A third equation,

$$1 = n_{\rightarrow,i} + n_{o,i} + \sum_{s=1}^{\ell} (n_{\times,i+s} + n_{\leftarrow,i+s}),$$

can be written because each lattice site is occupied by either a hole or some part of a particle. However, this third equation is linearly dependent on Eqs. 7 and 8.

We can use Eqs. 7 and 8 to eliminate $n_{\leftarrow,i}$ and $n_{o,i}$ from the problem, so we will write differential equations for the time evolution of only the two remaining types of densities, $n_{\rightarrow,i}$ and $n_{\times,i}$. Fluxes into and out of each state take the form of a product of the appropriate rate constant, the density of the state that may evolve, and the conditional probability that adjacent particles and holes are arranged appropriately for the evolution to occur. For example, a hole-hole pair at bond i will evolve to a particle-hole pair at bond i with rate

$$k_{i-1} n_{o,i} P(\bullet-o-o \mid ?-o-o).$$

We make mean field assumptions for the conditional probability, similar to that of MacDonald *et al.* [1]. For example,

$$\begin{aligned} P(\bullet-o-o \mid ?-o-o) &\approx P(\bullet-o-o \mid ?-o-?) \\ &= \frac{n_{\rightarrow,i-1}}{n_{\rightarrow,i-1} + n_{o,i-1}}. \end{aligned}$$

Thus the flux of hole-hole pairs at site i to particle-hole pairs at site i is

$$k_{i-1}n_{\circ,i}\frac{n_{\rightarrow,i-1}}{n_{\rightarrow,i-1}+n_{\circ,i-1}}$$

The resulting differential equations for time evolution of the bond densities in the bulk are

$$\frac{dn_{\rightarrow,i}}{dt} = k_{i+\ell}n_{\times,i}\frac{n_{\rightarrow,i+\ell}}{n_{\rightarrow,i+\ell}+n_{\times,i+\ell}} + k_{i-1}n_{\circ,i}\frac{n_{\rightarrow,i-1}}{n_{\rightarrow,i-1}+n_{\circ,i-1}} - k_in_{\rightarrow,i} \quad (9a)$$

$$\frac{dn_{\times,i}}{dt} = k_{i-1}n_{\leftarrow,i}\frac{n_{\rightarrow,i-1}}{n_{\rightarrow,i-1}+n_{\circ,i-1}} - k_{i+\ell}n_{\times,i}\frac{n_{\rightarrow,i+\ell}}{n_{\rightarrow,i+\ell}+n_{\times,i+\ell}}. \quad (9b)$$

We also have boundary conditions, and for convenience, we assume that particles enter the lattice one site at a time, so that only the first site must be free for initiation to occur. We also assume that a particle whose right edge is on site N can leave the lattice, freeing the final ℓ sites. Particle-particle bonds thus cannot exist in the final ℓ sites. Then the boundary conditions are, for initiation,

$$\begin{aligned} \frac{dn_{\rightarrow,1}}{dt} &= k_{1+\ell}n_{\times,1}\frac{n_{\rightarrow,1+\ell}}{n_{\rightarrow,1+\ell}+n_{\times,1+\ell}} + k_0n_{\circ,1} - k_1n_{\rightarrow,1} \\ \frac{dn_{\times,1}}{dt} &= k_0n_{\leftarrow,1} - k_{1+\ell}n_{\times,1}\frac{n_{\rightarrow,1+\ell}}{n_{\rightarrow,1+\ell}+n_{\times,1+\ell}} \end{aligned}$$

and, for $i = N - \ell + 1, \dots, N$,

$$\begin{aligned} \frac{dn_{\rightarrow,i}}{dt} &= k_{i-1}n_{\circ,i}\frac{n_{\rightarrow,i-1}}{n_{\rightarrow,i-1}+n_{\circ,i-1}} - k_in_{\rightarrow,i} \\ \frac{dn_{\times,i}}{dt} &= 0. \end{aligned}$$

It is possible to obtain an iterative steady state solution for the bond densities, from $i = N$ to $i = 1$. However, this solution appears to exhibit numerical instabilities in the high density regime that are similar to those observed with the original mean field theory. We would prefer to have a simple method, like the iteration and bisection method, for computing the current despite the numerical difficulties in computing the densities. However, such a method is not apparent. Instead, we begin with an empty lattice and directly integrate the differential equations for the bond densities (Eq. 9) until steady state is attained. The two-point mean field approach produces both densities and currents that agree more closely with Monte Carlo simulations than did the original (one-point) mean field theory. Table I compares two-point mean field currents with currents from Monte Carlo and the one-point mean field theory for real gene sequences. In each case, the two-point mean field does as well as or better than the original mean field at matching the Monte Carlo currents. Fig. 3 compares the two-point mean field density profile with that obtained by the other methods, showing that the two-point mean field theory successfully incorporates more of the long-range correlations than does the one-point mean field theory.

VI. CONCLUSIONS

We have considered one-dimensional driven lattice gas models with large particles and quenched disorder. Mean field theories were found to be effective in computing quantities of interest. The mean field equations originally proposed by MacDonald *et al.* [1, 2] for uniform systems were found to work equally well for nonuniform systems. An iterative method allowed easy and rapid computation of the steady state current through the system. Steady state particle densities were also computed by this method, although only when the system was in a low-density phase. We have gained some insight into the numerical difficulties that arise in obtaining high density solutions. Direct integration of differential equations for the time evolution of particle densities can always be used to find the steady state densities. We found good agreement between the mean field current and the Monte Carlo current. Agreement between the densities was also adequate, though not as good in the high density regime.

We extended the mean field approach to two-point correlations, using similar mean field approximations for conditional probabilities. Currents and particle densities were obtained more accurately from the two-point mean field theory than from the original.

Although the two-point mean field theory is an im-

provement on the original theory, Fig. 3 shows that it still does not capture all of the correlations necessary to reproduce high density profiles. The theory could be further extended to include three-point correlations (such as the density of particle-particle-hole triplets). However, the number of independent variables and equations, as well as the complexity of the equations, would increase as more correlations are added. Also, numerical instabilities might still exist so that solutions could be found only by integration. We therefore feel that it is not convenient to extend the method to include higher-order correlations.

We conclude that mean field approaches can be effective in studying disordered systems. If one is primarily interested in the current through the system, this quantity can be computed rapidly using iteration and bisection.

We expect the iteration and bisection method to be quite valuable in future studies, because the calculated protein production rates could be compared to experimental data (e.g., data in [5]) and used in fitting of unknown rate constants.

Acknowledgments

We thank Royce Zia for his helpful suggestions. KHL acknowledges support from the NSF through grants BES-0120315 and 9874938. LBS was supported by a Corning Foundation Fellowship and an IBM Ph.D. Fellowship.

-
- [1] C. MacDonald, J. Gibbs, and A. Pipkin, *Biopolymers* **6**, 1 (1968).
 - [2] C. MacDonald and J. Gibbs, *Biopolymers* **7**, 707 (1969).
 - [3] G. Lakatos and T. Chou, *J. Phys. A* **36**, 2027 (2003).
 - [4] L. Shaw, R. Zia, and K. Lee, *Phys. Rev. E* **68**, 021910 (2003).
 - [5] P. Lee, L. Shaw, L. Choe, A. Mehra, V. Hatzimanikatis, and K. Lee, *Biotech. and Bioeng.* **84**, 834 (2003).
 - [6] L. Stryer, *Biochemistry* (W.H. Freeman, New York, 1995), 4th ed.
 - [7] F. Neidhardt and H. Umbarger, in *Escherichia coli and Salmonella*, edited by F.C. Neidhardt (ASM Press, Washington, D.C., 1996), 2nd ed.
 - [8] R. Heinrich and T. Rapoport, *J. Theor. Biol.* **86**, 279 (1980).
 - [9] C. Kang and C. Cantor, *J. Mol. Biol.* **181**, 241 (1985).
 - [10] A. Bortz, M. Kalos, and J. Lebowitz, *J. Comp. Phys.* **17**, 10 (1975).
 - [11] *E. coli* Genome Project at the University of Wisconsin-Madison, <http://www.genome.wisc.edu/sequencing/k12.htm>
 - [12] J. Solomovici, T. Lesnik, and C. Reiss, *J. Theor. Biol.* **185**, 511 (1997).
 - [13] T. Lesnik, J. Solomovici, A. Deana, R. Erhlich, and C. Reiss, *J. Theor. Biol.* **202**, 175 (2000).
 - [14] B. Derrida, E. Domany, and D. Mukamel, *J. Stat. Phys.* **69**, 667 (1992).
 - [15] G. Schütz and E. Domany, *J. Stat. Phys.* **72**, 277 (1993).
 - [16] V. Popkov and G. Schütz, *Europhys. Lett.* **48**, 257 (1999).
 - [17] A. Kolomeisky, G. Schütz, E. Kolomeisky, and J. Straley, *J. Phys. A* **31**, 6911 (1998).
 - [18] B. Derrida, *J. Stat. Phys.* **31**, 433 (1983). For generalizations and more recent studies see, e.g., A. Kolomeisky and M. Fisher, *J. Chem. Phys.*, **113**, 10867 (2000) and references therein.
 - [19] S. Janowsky and J. Lebowitz, *Phys. Rev. A* **45**, 618 (1992).
 - [20] S. Janowsky and J. Lebowitz, *J. Stat. Phys.* **77**, 35 (1994).
 - [21] T. Seppäläinen, *J. Stat. Phys.* **102**, 69 (2001).
 - [22] A. Kolomeisky, *J. Phys. A* **31**, 1153 (1998).
 - [23] G. Tripathy and M. Barma, *Phys. Rev. E* **58**, 1911 (1998).
 - [24] J. Krug., *Brazilian J. Phys.* **30**, 97 (2000); cond-mat/9912411.
 - [25] L. Shaw, A. Kolomeisky, and K. Lee, *J. Phys. A* **37**, 2105 (2004).